

Spectral and energy efficiency analysis for massive MIMO multi-pair two-way relaying networks under generalized power scaling

Jing YANG^{1,2*}, Hongyan WANG², Jie DING², Xiqi GAO¹ & Zhiguo DING³

¹National Mobile Communications Research Laboratory, Southeast University, Nanjing 210096, China;

²School of Information Engineering, Yangzhou University, Yangzhou 225009, China;

³Department of Communication Systems, Lancaster University, Lancaster LA1 4YW, UK

Received October 21, 2016; accepted November 28, 2016; published online March 13, 2017

Abstract In this work, we investigate the spectral efficiency (SE) and energy efficiency (EE) for a massive multiple-input multiple-output multi-pair two-way amplify-and-forward relaying system, where multi-pair users exchange information via a relay station equipped with large scale antennas. We assume that imperfect channel state information is available and maximum-ratio combining/maximum-ratio transmission beamforming is adopted at the relay station. Considering constant or scaled transmit power of pilot sequences, we quantify the asymptotic SE and EE under general power scaling schemes, in which the transmit power at each user and relay station can both be scaled down, as the number of relay antennas tends to infinity. In addition, a closed-form expression of the SE has been obtained approximately. Our results show that by using massive relay antennas, the transmit power at each user and the relay station can be scaled down, with a non-vanishing signal to interference and noise ratio (SINR). Finally, simulation results confirm the validity of our analysis.

Keywords massive MIMO, two-way relaying, power scaling, imperfect CSI, energy efficiency, spectral efficiency

Citation Yang J, Wang H Y, Ding J, et al. Spectral and energy efficiency analysis for massive MIMO multi-pair two-way relaying networks under generalized power scaling. *Sci China Inf Sci*, 2017, 60(10): 102303, doi: 10.1007/s11432-016-9007-2

1 Introduction

In the massive multiple-input multiple-output (MIMO) systems, the base station (BS) deployed hundreds or more antennas can serve tens of user terminals in the same time-frequency resource, achieving higher dramatic data rate and power efficiency [1–3]. It was shown that when the antenna number at BS, i.e., N , increases sufficiently large, the detrimental effects in the conventional wireless systems, such as inter-pair interference, small-scale fading and noise, will totally clear away through some simple linear processing approaches [3, 4]. Furthermore, massive MIMO can remarkably boost the energy efficiency (EE) of the system, for instance, the transmit power of each antenna can be scaled down by $1/N$ or $1/\sqrt{N}$ maintaining a desirable rate, depending on availability of the channel state information (CSI)

* Corresponding author (email: jingyang@yzu.edu.cn)

at the BS [3, 5–7]. These attractive features make massive MIMO gain significant interest from both academia and industry, and understanding the fundamental performance limits of the massive MIMO systems has become a hot topic.

On the other hand, the two-way relaying inherits the benefits of the one-way relaying for capturing higher capacity, longer network lifetime and so on, meanwhile it effectively utilizes the spectrum resources [8, 9]. Two-way relaying system combined with massive MIMO can be regarded as a promising technique to remarkably improve the performance, e.g., spectral efficiency (SE) and EE [10–13]. With variable gain AF relaying adopted, Cui et al. [10] investigated the asymptotic SE and EE for the specific power-scaling schemes. With fixed gain amplify-and-forward (AF) relaying utilized, Jin et al. [11] studied the ergodic rates and EE for a massive MIMO two-way relaying system. In [12], a power allocation scheme was proposed to maximize the sum SE in the massive MIMO two-way AF relaying system. Achievable rate was studied for the massive MIMO two-way decode-and-forward relaying system [13]. The above works assumed perfect CSI is available.

However, massive MIMO still has many challenges we have to deal with. A fundamental one is to acquire accurate CSI at the BS [14]. In [15], the authors investigated the resource allocation problem for a pilot-assisted multi-user massive MIMO uplink with linear minimum mean-squared error (MMSE) channel estimation and detection. Moreover, some studies on massive MIMO with imperfect CSI have been presented [16–21]. Considering the multiuser massive MIMO downlink transmission, Khansefid et al. [16] maximized the sum-rate lower bound with an asymptotic optimal power allocation, and Dong et al. [17] derived a closed-form lower bound on the area spectral efficiency. Considering the uplink massive MIMO systems, considering the most dominant factor of large-scale fading, Yang et al. [18] obtained a novel expression on the asymptotic ergodic achievable rate; the authors in [20] investigated the achievable sum-rate with aged CSI. For the massive MIMO two-way relaying system, we studied the asymptotic signal to interference and noise ratio (SINR) with zero-forcing beamforming adopted at the relay station with imperfect CSI; and the authors in [21] studied the impact of co-channel interference and the pilot contamination. However, in the above studies [10, 13, 16–19, 21], only specific power scaling schemes for the transmit power at each user, i.e., P_U and at the relay station, i.e., P_R , are considered, for example, $P_U = E_U/N, P_R = E_R/N$, where E_U and E_R are constant values, and N is the antenna number at the relay station [21]. Focusing on the uplink massive system, the authors in [20] investigated a general power scaling scheme.

Different from the existing works, i.e., [10, 13, 16–19, 21], we investigate the SE and EE in a massive MIMO two-way AF relaying system, assuming the general power scaling schemes are used at the each user and the relay station. Specifically, we define $P_U = \frac{E_U}{N^a}, P_R = \frac{E_R}{N^b}$, and $a \geq 0, b \geq 0$, indicating the power scaling laws at the each user and relay station, respectively. Furthermore, we consider two cases for the transmit power of pilot sequences P_P , i.e., $P_P = c$ where c is a constant, and $P_P = \tau P_U$ indicating P_P is scaled down proportionally to N^a . The first case is called fixed P_P case, and the latter is called variable P_P case in this paper. In addition, we assume maximum-ratio combining/maximum-ratio transmission (MRC/MRT) beamforming is adopted at the relay station, and imperfect CSI is available. We derive the general asymptotic SINR at the k 'th user when $N \rightarrow \infty$, from which the asymptotic SE and EE is obtained analytically. Additionally, the approximate closed-form expression on the SE in the considered system is also obtained. It is shown that the analytical results in [10] are the special cases of our results. Our analytical results in this paper show that the transmit power at each user, i.e., P_U , and at the relay transmit power, i.e., P_R , and/or the transmit power of pilot sequences P_P , can be dramatically reduced without the loss in the system performance. Finally, Monte-Carlo simulations are employed to verify these results.

Notation. $\|\cdot\|, (\cdot)^T, (\cdot)^*, (\cdot)^H, (\cdot)^{-1}$ and $\text{Tr}(\cdot)$ represent the Euclidean norm, the transpose, the conjugate, the conjugate transpose, the inverse, and the trace of a matrix, respectively. $E\{\mathbf{x}\}$ stands for the expectation of a random variable \mathbf{x} and \mathbf{I}_N denotes an $N \times N$ identity matrix. $\mathbf{1}_i, (i = 1, \dots, 2K)$ represents the i th entry is 1 in a $1 \times 2K$ vector, and the others are 0; $\delta_{ki} = 1$ if $k = i$, and $\delta_{ki} = 0$, otherwise. $\mathbf{0}_{2K \times 1}$ is a zero $2K \times 1$ vector. $\mathbf{1}_N$ is a $N \times 1$ vector where all elements are 1. $\mathcal{CN}(\mu, \sigma_n^2)$

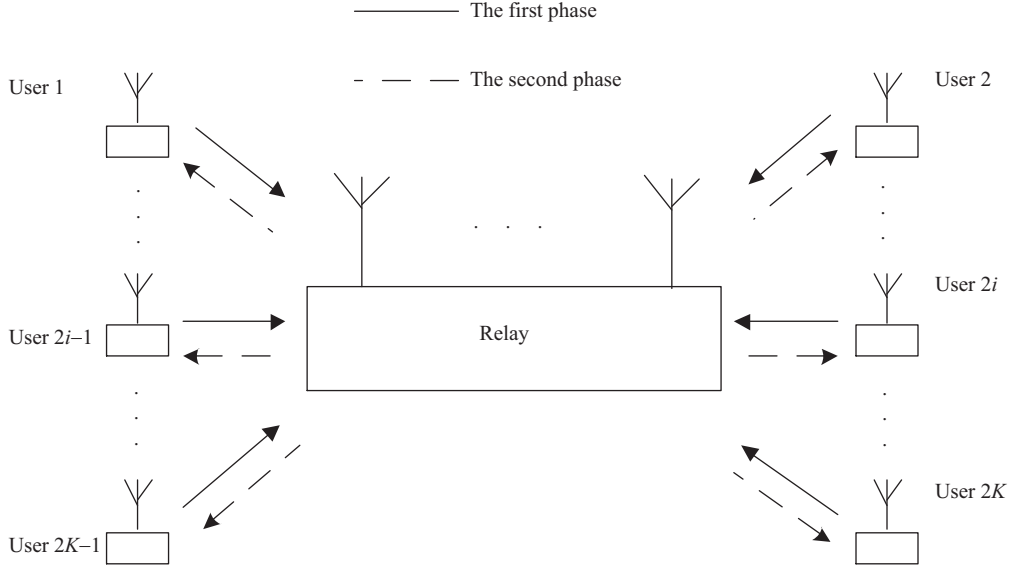


Figure 1 The system model of the multi-pair massive MIMO two-way AF relaying system.

is the complex-Gaussian distribution with mean μ and variance σ_n^2 . $\xrightarrow[N \rightarrow \infty]{\text{a.s.}}$ represents the almost sure convergence, when N approaches to infinity, and $\xrightarrow[N \rightarrow \infty]{d}$ denotes the convergence in distribution, when N approaches to infinity.

2 System model

As illustrated in Figure 1, in a multi-pair two-way relaying system, $2K$ users comprising K communication pairs exchange information with each other within a pair, with the help of a shared AF relay station. The relay station is equipped with N ($N \geq 2K$) antennas while each user has a single antenna. Consider users k and k' as a communication pair (k, k') , in which they exchange information with each other. Thus, the i th communication pair can be denoted by $(2i - 1, 2i), i = 1, \dots, K$. The channel matrix between the relay station and $2K$ users is denoted by $\mathbf{G} = [\mathbf{g}_1, \dots, \mathbf{g}_{2K}] \in \mathbb{C}^{N \times 2K}$, with $\mathbf{g}_k \sim \mathcal{CN}(0, \eta_k \mathbf{1}_N)$ representing the channel between the k th user and the relay station. Furthermore, the channel matrix is modeled as $\mathbf{G} = \mathbf{H}\mathbf{D}^{1/2}$, where $\mathbf{H} \in \mathbb{C}^{N \times 2K}$ denotes the normalized small-scale fading matrix between the relay station and all users, following independent identically distributed (i.i.d.) Rayleigh fading, and $\mathbf{D} \in \mathbb{C}^{2K \times 2K}$ is the diagonal large-scale fading matrix with $[\mathbf{D}]_{kk} = \eta_k$, representing the large-scale fading coefficient. Channel reciprocity is assumed in this paper.

2.1 Channel estimation

Before data transmission, channel estimation is performed during the training part of the coherence interval. Assume that the relay station performs minimum mean squared error (MMSE) channel estimation by transmitting the orthogonal pilot sequences [13, 22]. Thus, the received pilot matrix at the relay station is given by

$$\mathbf{Y}_P = \sqrt{P_P} \mathbf{G} \Phi^T + \mathbf{N}, \quad (1)$$

where P_P denotes the transmit power, $\Phi \in \mathbb{C}^{\tau \times 2K}$ represents the pilot sequences from all the users to the relay station satisfying $\Phi^H \Phi = \mathbf{I}_{2K}$, τ ($\tau \geq 2K$) is the length of the pilot sequences, and $\mathbf{N} \in \mathbb{C}^{N \times \tau}$ denotes the additive white AWGN matrix with i.i.d. $\mathcal{CN}(0, 1)$ elements.

Then, the MMSE channel estimation $\hat{\mathbf{G}}$ of \mathbf{G} , which is the true channel matrix, is expressed as [13]

$$\hat{\mathbf{G}} = \frac{1}{\sqrt{P_P}} \mathbf{Y}_P \Phi^* \tilde{\mathbf{D}} = \left(\mathbf{G} + \frac{1}{\sqrt{P_P}} \mathbf{W} \right) \tilde{\mathbf{D}}, \quad (2)$$

where $\mathbf{W} = \mathbf{N}\Phi^*$, and $\tilde{\mathbf{D}} \triangleq (\frac{1}{P_P}\mathbf{D}^{-1} + \mathbf{I}_{2K})^{-1}$. Since $\Phi^H\Phi = \mathbf{I}_{2K}$, the elements of \mathbf{W} follow $\mathcal{CN}(0, 1)$.

Recalling $\mathbf{g}_k \sim \mathcal{CN}(0, \eta_k \mathbf{1}_N)$, $\mathbf{g}_{k'} \sim \mathcal{CN}(0, \eta_{k'} \mathbf{1}_N)$ and according to the large number law [23], we have

$$\frac{1}{N}\mathbf{g}_k^H \mathbf{g}_k \xrightarrow[N \rightarrow \infty]{\text{a.s.}} \eta_k, \quad \frac{1}{N}\mathbf{g}_k^H \mathbf{g}_{k'} \xrightarrow[N \rightarrow \infty]{\text{a.s.}} 0, \quad (3)$$

yielding

$$\frac{1}{N}\hat{\mathbf{G}}^H \hat{\mathbf{G}} \xrightarrow[N \rightarrow \infty]{\text{a.s.}} \tilde{\mathbf{D}}^H \mathbf{D} \tilde{\mathbf{D}} + \frac{1}{P_P}\tilde{\mathbf{D}}^H \tilde{\mathbf{D}} = \hat{\mathbf{\Lambda}}, \quad (4)$$

where $[\hat{\mathbf{\Lambda}}]_{kk} = \frac{P_P \eta_k^2}{P_P \eta_k + 1}$. Therefore, the elements of $\hat{\mathbf{g}}_k \sim \mathcal{CN}(0, \frac{P_P \eta_k^2}{P_P \eta_k + 1})$.

Let \mathbf{E} be the error matrix and assume the orthogonality between $\hat{\mathbf{G}}$ and \mathbf{E} . Thus, we have [13]

$$\mathbf{G} = \hat{\mathbf{G}} + \mathbf{E}, \quad (5)$$

where $\mathbf{e}_k \sim \mathcal{CN}(0, \sigma_{e_k}^2 \mathbf{1}_N)$ is the k th column of \mathbf{E} which is independent of the k th column of $\hat{\mathbf{G}}$. Recalling $\mathbf{g}_k \sim \mathcal{CN}(0, \eta_k \mathbf{1}_N)$ and $\hat{\mathbf{g}}_k \sim \mathcal{CN}(0, \frac{P_P \eta_k^2}{P_P \eta_k + 1} \mathbf{1}_N)$, one can obtain

$$\sigma_{e_k}^2 = \frac{\eta_k}{P_P \eta_k + 1}. \quad (6)$$

2.2 Data transmission

The whole data transmission takes place in two phases, i.e., the multiple-access (MA) phase and the broadcast (BC) phase. During the MA phase, all $2K$ users simultaneously transmit their respective information to the relay station. Thus, the received signal $\mathbf{y}_r \in \mathbb{C}^{N \times 1}$ at the relay station can be expressed as

$$\mathbf{y}_r = \sum_{i=1}^{2K} \mathbf{g}_i \sqrt{P_U} x_i + \mathbf{n}_r = \sqrt{P_U} \mathbf{G} \mathbf{x} + \mathbf{n}_r, \quad (7)$$

where $\mathbf{x} = [x_1, \dots, x_{2K}]^T$ stands for the transmitted symbols with $\mathbb{E}\{\mathbf{x}\mathbf{x}^H\} = \mathbf{I}_{2K}$, $\mathbf{n}_r \in \mathbb{C}^{N \times 1}$ represents the zero-mean AWGN at the relay station with $\mathbb{E}\{\mathbf{n}_r \mathbf{n}_r^H\} = \sigma_n^2 \mathbf{I}_N$, and P_U is the transmit power at each user.

During the BC phase, the relay station broadcasts the amplified signal $\mathbf{y} = \mathbf{F} \mathbf{y}_r$ to the $2K$ users, where $\mathbf{F} \in \mathbb{C}^{N \times N}$ denotes the MRC/MRT beamforming matrix at the relay station. Utilizing the channel estimate $\hat{\mathbf{G}}$, the beamforming matrix \mathbf{F} is given as follows [10]:

$$\mathbf{F} = \beta \hat{\mathbf{G}}^* \mathbf{P} \hat{\mathbf{G}}^H, \quad (8)$$

where β is the amplification factor to satisfy power constraint at the relay station, and $\mathbf{P} = \text{diag}\{\mathbf{P}_1, \dots, \mathbf{P}_K\}$ is the block diagonal matrix, following $\mathbf{P}_i = [0 \ 1; 1 \ 0]$, $i = 1, \dots, K$. Specifically, β is given by [11]

$$\beta = \sqrt{\frac{P_R}{P_U \text{Tr}(\mathbf{Z}_1) + \sigma_n^2 \text{Tr}(\mathbf{Z}_2)}}, \quad (9)$$

where $\mathbf{Z}_1 = \hat{\mathbf{G}}^* \mathbf{P} \hat{\mathbf{G}}^H \hat{\mathbf{G}} \mathbf{P} \hat{\mathbf{G}}^T$ and $\mathbf{Z}_2 = \hat{\mathbf{G}}^* \mathbf{P} \hat{\mathbf{G}}^H (\hat{\mathbf{G}} + \mathbf{E})(\hat{\mathbf{G}}^H + \mathbf{E}^H) \hat{\mathbf{G}} \mathbf{P} \hat{\mathbf{G}}^T$. Therefore, the received signal at the k' th user is given by

$$y_{k'} = \mathbf{g}_{k'}^T \mathbf{y} + n_{k'} = \mathbf{g}_{k'}^T \mathbf{F} \mathbf{g}_k \sqrt{P_U} x_k + \mathbf{g}_{k'}^T \mathbf{F} \mathbf{g}_{k'} \sqrt{P_U} x_{k'} + \mathbf{g}_{k'}^T \mathbf{F} \sum_{i \neq k, k'}^{2K} \mathbf{g}_i \sqrt{P_U} x_i + \mathbf{g}_{k'}^T \mathbf{F} \mathbf{n}_r + n_{k'}, \quad (10)$$

where $n_{k'} \sim \mathcal{CN}(0, \sigma_n^2)$ is the AWGN at the k' th user.

After canceling the self-interference term $\mathbf{g}_{k'}^T \mathbf{F} \mathbf{g}_{k'} \sqrt{P_U} x_{k'}$ in (10), and substituting (5) into (10), the remaining received signal at the k' th user is given by

$$y_{c,k'} = \underbrace{\mathbf{g}_{k'}^T \mathbf{F} \hat{\mathbf{g}}_k \sqrt{P_U} x_k}_{\text{signal}} + \underbrace{\mathbf{g}_{k'}^T \mathbf{F} \mathbf{e}_k \sqrt{P_U} x_k + \mathbf{e}_{k'}^T \mathbf{F} \hat{\mathbf{g}}_k \sqrt{P_U} x_k}_{\text{(additional noise)}} \quad (11)$$

$$\begin{aligned}
 & + \underbrace{e_{k'}^T \mathbf{F} e_k \sqrt{P_U x_k}}_{\text{(additional noise)}} + \underbrace{\hat{\mathbf{g}}_{k'}^T \mathbf{F} e_{k'} \sqrt{P_U x_{k'}} + e_{k'}^T \mathbf{F} \hat{\mathbf{g}}_{k'} \sqrt{P_U x_{k'}} + e_{k'}^T \mathbf{F} e_{k'} \sqrt{P_U x_{k'}}}_{\text{(residual self-interference)}} \\
 & + \underbrace{(\hat{\mathbf{g}}_{k'}^T + e_{k'}^T) \mathbf{F} \sum_{i \neq k, k'}^{2K} (\hat{\mathbf{g}}_i + e_i) \sqrt{P_U x_i}}_{\text{(inter-pair interference)}} + \underbrace{(\hat{\mathbf{g}}_{k'}^T + e_{k'}^T) \mathbf{F} \mathbf{n}_r + n_{k'}}_{\text{(noise)}}.
 \end{aligned}$$

From (11), it can be seen that the residual self-interference and additional noise are introduced due to the channel estimation errors.

Consequently, the received SINR at the k' th user is expressed as

$$\gamma_{k'} = \frac{P_U |\hat{\mathbf{g}}_{k'}^T \mathbf{F} \hat{\mathbf{g}}_k|^2}{P_A + P_{SI} + P_{II} + P_N}, \quad (12)$$

where

$$P_A = P_U (|\hat{\mathbf{g}}_{k'}^T \mathbf{F} e_k|^2 + |e_{k'}^T \mathbf{F} \hat{\mathbf{g}}_k|^2 + |e_{k'}^T \mathbf{F} e_k|^2),$$

$$P_{SI} = P_U (|\hat{\mathbf{g}}_{k'}^T \mathbf{F} e_{k'}|^2 + |e_{k'}^T \mathbf{F} \hat{\mathbf{g}}_{k'}|^2 + |e_{k'}^T \mathbf{F} e_{k'}|^2),$$

$$P_{II} = P_U \sum_{i \neq k, k'}^{2K} (|\hat{\mathbf{g}}_{k'}^T \mathbf{F} \hat{\mathbf{g}}_i|^2 + |\hat{\mathbf{g}}_{k'}^T \mathbf{F} e_i|^2 + |e_{k'}^T \mathbf{F} \hat{\mathbf{g}}_i|^2 + |e_{k'}^T \mathbf{F} e_i|^2),$$

and

$$P_N = \sigma_n^2 (\|\hat{\mathbf{g}}_{k'}^T \mathbf{F}\|^2 + \|e_{k'}^T \mathbf{F}\|^2) + \sigma_n^2$$

represent the power of the additional noise, the residual self-interference, the inter-pair interference and AWGN, respectively.

From (12), the SE of the massive MIMO multi-pair two-way relaying system is defined as [11]

$$R_{\text{sum}} = \frac{T - \tau}{2T} \mathbb{E} \left[\sum_{i=1}^{2K} \log_2 (1 + \gamma_i) \right], \quad (13)$$

where T denotes the coherence interval time, and the coefficient $1/2$ is because the data transmission within a communication pair takes place in two phases. Therefore, the EE of the considered system is defined as [11]

$$\rho = \frac{R_{\text{sum}}}{2K P_U + P_R}, \quad (14)$$

where $2K P_U + P_R$ denotes the total power consumption at all users and the relay station.

3 Asymptotic SINR for different power scaling cases

In this section, we investigate how much power can be scaled down at each user and the relay station with a non-vanishing SINR, as $N \rightarrow \infty$. Rewrite $P_U = \frac{E_U}{N^a}$, $P_R = \frac{E_R}{N^b}$, where E_U and E_R are constants, $a \geq 0$ and $b \geq 0$ indicate the power scaling laws at the each user and the relay station, respectively. For variable P_P , $P_P = \tau P_U$ indicates that the transmit power of pilot sequences is also scaled down by $1/N^a$; for fixed P_P , $P_P = c$, where c is a constant. The asymptotic SINR at the k' th user is firstly derived for fixed and variable P_P , respectively, from which the asymptotic SE and EE can be obtained analytically.

3.1 Asymptotic SINR at the k' th User with Fixed P_P , $P_P = c$

With the fixed transmit power of pilot sequences, i.e., $P_P = c$, the asymptotic SINR at the k' th user is presented in the following Theorem 1.

Theorem 1. With the fixed transmit power of pilot sequences, i.e., $P_P = c$, and $P_U = \frac{E_U}{N^a}$, $P_R = \frac{E_R}{N^b}$, $a, b \geq 0$, for fixed E_U and E_R , the asymptotic SINR at the k' th user is given by

$$\gamma_{k'} \xrightarrow[N \rightarrow \infty]{\text{a.s.}} \frac{E_U E_R (\eta_k - \sigma_{e_k}^2)^2 (\eta_{k'} - \sigma_{e_{k'}}^2)^2 N^{2-a-b}}{E_R (\eta_k - \sigma_{e_k}^2) (\eta_{k'} - \sigma_{e_{k'}}^2)^2 \sigma_n^2 N^{1-b} + E_U \varphi_2 \sigma_n^2 N^{1-a} + \varphi_1 \sigma_n^4}, \quad (15)$$

where

$$\varphi_1 = 2 \sum_{i=1}^K (\eta_{2i-1} - \sigma_{e_{2i-1}}^2) (\eta_{2i} - \sigma_{e_{2i}}^2) \quad (16)$$

and

$$\varphi_2 = \sum_{i=1}^K (\eta_{2i-1} - \sigma_{e_{2i-1}}^2) (\eta_{2i} - \sigma_{e_{2i}}^2) \left[(\eta_{2i-1} - \sigma_{e_{2i-1}}^2) + (\eta_{2i} - \sigma_{e_{2i}}^2) \right]. \quad (17)$$

Proof. See Appendix A.

Remark 1. Theorem 1 implies that for a non-vanishing $\gamma_{k'}$ as $N \rightarrow \infty$, we should have $2 - a - b \geq \max(1 - b, 0, 1 - a)$, or equivalently $0 \leq a, b \leq 1$. As such, $\gamma_{k'}$ increases as N grows without bound. With $P_P = c$, the transmit power at each user and relay station can be both further scaled down by $1/N$, maintaining a constant $\gamma_{k'}$ as $N \rightarrow \infty$. In particular, $\gamma_{k'}$ converges to the constant for the following three cases: $2 - a - b = 3 - b > \max(0, 1 - a)$, $2 - a - b = 1 - a > \max(1 - b, 0)$ and $2 - a - b = 1 - b = 0 = 1 - a$, or equivalently $(a = 1, 0 \leq b < 1)$, $(0 \leq a < 1, b = 1)$, and $(a = b = 1)$, respectively. Specially, we have the cases as follows.

- Case A-I ($a = 1, 0 \leq b < 1$):

$$\gamma_{k'} \xrightarrow[N \rightarrow \infty]{\text{a.s.}} \gamma_{f1,k'}^{\text{asm}} = \frac{E_U (\eta_k - \sigma_{e_k}^2)}{\sigma_n^2}. \quad (18)$$

- Case A-II ($0 \leq a < 1, b = 1$):

$$\gamma_{k'} \xrightarrow[N \rightarrow \infty]{\text{a.s.}} \gamma_{f2,k'}^{\text{asm}} = \frac{E_R (\eta_{k'} - \sigma_{e_{k'}}^2)^2 (\eta_k - \sigma_{e_k}^2)^2}{\varphi_2 \sigma_n^2}. \quad (19)$$

- Case A-III ($a = b = 1$):

$$\gamma_{k'} \xrightarrow[N \rightarrow \infty]{\text{a.s.}} \frac{\gamma_{f1,k'}^{\text{asm}} \gamma_{f2,k'}^{\text{asm}}}{\gamma_{f1,k'}^{\text{asm}} + \gamma_{f2,k'}^{\text{asm}} + \varphi_1 / \varphi_2}. \quad (20)$$

In Case A-I, the asymptotic SINR is only limited by the channel estimation error, the average signal noise ratio (SNR) and the large-scale fading. In addition, with the increase of N , the AWGN at the k' th user converges to zero. While in Case A-II and Case A-III, the AWGNs at each user and the relay station do not tend to zero when $N \rightarrow \infty$. Moreover, when $E_R \rightarrow \infty$, $\gamma_{f3,k'}^{\text{asm}}$ runs to the asymptotic SINR in Case A-I, i.e., $\gamma_{f1,k'}^{\text{asm}}$ in (18); and when $E_U \rightarrow \infty$, $\gamma_{f3,k'}^{\text{asm}}$ runs to the asymptotic SINR in Case A-II, i.e., $\gamma_{f2,k'}^{\text{asm}}$ in (19).

Remark 2. In particular, when the system structure is symmetric, i.e., $\eta_i = 1$, $\sigma_{e_i}^2 = \sigma_e^2$, $i = 1, \dots, 2K$, and $E_U = E_R = E$, the asymptotic SINR $\gamma_{k'}$ in (15) becomes

$$\gamma_{k'} \xrightarrow[N \rightarrow \infty]{\text{a.s.}} \frac{E^2 (1 - \sigma_e^2)^2 N^{2-a-b}}{E (1 - \sigma_e^2)^2 \sigma_n^2 N^{1-b} + 2KE (1 - \sigma_e^2) \sigma_n^2 N^{1-a} + 2K \sigma_n^4}. \quad (21)$$

Accordingly, Eqs. (18)–(20) become

$$\gamma_{f1,k'}^{\text{asm}} = \frac{E(1 - \sigma_e^2)}{\sigma_n^2}, \quad \gamma_{f2,k'}^{\text{asm}} = \frac{E(1 - \sigma_e^2)}{2K\sigma_n^2}$$

and

$$\gamma_{f3,k'}^{\text{asm}} = \frac{\gamma_{sf1,k'}^{\text{asm}} \gamma_{sf2,k'}^{\text{asm}}}{\gamma_{f1,k'}^{\text{asm}} + \gamma_{f2,k'}^{\text{asm}} + 1/(1 - \sigma_e^2)},$$

respectively.

Comparing $\gamma_{f1,k'}^{\text{asm}}$, $\gamma_{f2,k'}^{\text{asm}}$ and $\gamma_{f3,k'}^{\text{asm}}$ and considering the fact that $\frac{xy}{x+y+z} < \frac{xy}{x+y} \leq \min\{x, y\}$, where $x, y, z > 0$, it can be concluded that in the symmetric system, the asymptotic SINR in Case A-I is the maximal, while in Case A-III is the minimal among the three cases. Thus, the asymptotic SE in Case A-I is the greatest, and in Case A-III is the smallest. In addition, from (14), it can be observed that the asymptotic EE in Case A-III increases linearly with N . So, the asymptotic EE in Case A-III is the maximal in the above three cases.

Remark 3. With perfect CSI, we have $\sigma_{e_k}^2 = \frac{\eta_k}{P_P \eta_k + 1} \rightarrow 0$. In this case, $\gamma_{k'}$ in (15) becomes

$$\gamma_{k'} \xrightarrow[N \rightarrow \infty]{\text{a.s.}} \frac{E_U E_R \eta_k^2 \eta_{k'}^2 N^{2-a-b}}{E_R \eta_k \eta_{k'}^2 \sigma_n^2 N^{1-b} + E_U \sum_{i=1}^K \eta_{2i-1} \eta_{2i} (\eta_{2i-1} + \eta_{2i}) \sigma_n^2 N^{1-a} + 2 \sum_{i=1}^K \eta_{2i-1} \eta_{2i} \sigma_n^4}. \quad (22)$$

Furthermore, we note that, with perfect CSI, i.e., $\sigma_{e_k}^2 = \sigma_{e_{k'}}^2 = 0$, $\gamma_{f1,k'}^{\text{asm}}$, $\gamma_{f2,k'}^{\text{asm}}$ and $\gamma_{f3,k'}^{\text{asm}}$ in (18)–(20) reduce to the previously known results, i.e., [10, Eqs. (13), (20), (24)], respectively.

3.2 Asymptotic SINR at the k' th User with variable P_P , $P_P = \tau E_U / N^a, a \geq 0$

For variable P_P , i.e., $P_P = \tau P_U$, the asymptotic SINR at the k' th user is presented in the following Theorem 2.

Theorem 2. With the variable P_P , i.e., $P_P = \tau P_U$, and $P_U = \frac{E_U}{N^a}$, and $P_R = \frac{E_R}{N^b}$, where E_U and E_R are fixed, and $a \geq 0, b \geq 0$, as $N \rightarrow \infty$, the asymptotic SINR at the k' th user is given by

$$\gamma_{k'} \xrightarrow[N \rightarrow \infty]{\text{a.s.}} \frac{E_R \tau^2 E_U^3 \eta_k^4 \eta_{k'}^4 N^{2-3a-b}}{\tau E_R E_U \sigma_n^2 \eta_k^2 \eta_{k'}^4 N^{1-a-b} + \tau E_U^2 \sigma_n^2 \sum_{i=1}^K \eta_{2i-1}^2 \eta_{2i}^2 (\eta_{2i-1}^2 + \eta_{2i}^2) N^{1-2a} + 2 \sum_{i=1}^K \eta_{2i-1}^2 \eta_{2i}^2 \sigma_n^4}. \quad (23)$$

Proof. Recalling (6), φ_1 and φ_2 in (16) and (17) can be re-expressed as

$$\varphi_1 = 2 \sum_{i=1}^K \frac{P_P^2 \eta_{2i-1}^2 \eta_{2i}^2}{(P_P \eta_{2i-1} + 1)(P_P \eta_{2i} + 1)} \quad (24)$$

and

$$\varphi_2 = \sum_{i=1}^K \frac{P_P^3 \eta_{2i-1}^2 \eta_{2i}^2}{(P_P \eta_{2i-1} + 1)(P_P \eta_{2i} + 1)} \left(\frac{\eta_{2i-1}^2}{P_P \eta_{2i-1} + 1} + \frac{\eta_{2i}^2}{P_P \eta_{2i} + 1} \right), \quad (25)$$

respectively.

Due to (6), we have $\eta_k - \sigma_{e_k}^2 = \frac{P_P \eta_k^2}{P_P \eta_k + 1}$. Let $P_P = \tau P_U, P_U = \frac{E_U}{N^a}, P_R = \frac{E_R}{N^b}, a, b \geq 0$, thus $P_P \eta_k \ll 1$ as $N \rightarrow \infty$. Substituting (24) and (25) into (15), Theorem 2 can be easily achieved.

Remark 4. Theorem 2 implies that with a non-vanishing $\gamma_{k'}$ as $N \rightarrow \infty$, we should have $2 - 3a - b \geq \max(1 - a - b, 1 - 2a, 0)$, or equivalently, $0 \leq a \leq 1/2$ and $a + b \leq 1$. In particular, as $N \rightarrow \infty$, $\gamma_{k'}$ converges to the constant if $2 - 3a - b = \max(1 - a - b, 1 - 2a, 0)$, and equivalently ($a = 1/2, 0 \leq b < 1/2$), ($0 \leq a < 1/2, a + b = 1$), or ($a = b = 1/2$). Specially, we have the cases as follows.

- Case B-I ($a = 1/2, 0 \leq b < 1/2$):

$$\gamma_{k'} \xrightarrow[N \rightarrow \infty]{\text{a.s.}} \gamma_{v1,k'}^{\text{asm}} = \frac{\tau E_U^2 \eta_k^2}{\sigma_n^2}. \quad (26)$$

- Case B-II ($0 \leq a < 1/2$, $a + b = 1$):

$$\gamma_{k'} \xrightarrow[N \rightarrow \infty]{\text{a.s.}} \gamma_{v2,k'}^{\text{asm}} = \frac{\tau E_R E_U \eta_k^4 \eta_{k'}^4}{\sigma_n^2 \sum_{i=1}^K \eta_{2i-1}^2 \eta_{2i}^2 (\eta_{2i-1}^2 + \eta_{2i}^2)}. \quad (27)$$

- Case B-III ($a = b = 1/2$):

$$\gamma_{k'} \xrightarrow[N \rightarrow \infty]{\text{a.s.}} \gamma_{v3,k'}^{\text{asm}} = \frac{E_R \tau^2 E_U^3 \eta_k^4 \eta_{k'}^4}{\tau E_R E_U \sigma_n^2 \eta_k^2 \eta_{k'}^4 + \tau E_U^2 \sigma_n^2 \sum_{i=1}^K \eta_{2i-1}^2 \eta_{2i}^2 (\eta_{2i-1}^2 + \eta_{2i}^2) + 2\sigma_n^4 \sum_{i=1}^K \eta_{2i-1}^2 \eta_{2i}^2}. \quad (28)$$

Remark 5. With a constant $\gamma_{k'}$, as $N \rightarrow \infty$, the transmit power for the pilot sequences and data signal at each user can be scaled down simultaneously up to by $1/\sqrt{N}$, which leads to the so-called “squaring effect” [5, 6].

Remark 6. When the system structure is symmetric, i.e., $\eta_i = 1$, $\sigma_{e_i}^2 = \sigma_e^2$, $i = 1, \dots, 2K$, and $E_U = E_R = E$, the asymptotic SINR $\gamma_{k'}$ in (23) becomes

$$\gamma_{k'} \xrightarrow[N \rightarrow \infty]{\text{a.s.}} \frac{\tau^2 E^4 N^{2-3a-b}}{\tau E^2 \sigma_n^2 N^{1-a-b} + 2K \tau E^2 \sigma_n^2 N^{1-2a} + 2K \sigma_n^4}. \quad (29)$$

Therefore, Eqs. (26)–(28) become

$$\gamma_{v1,k'}^{\text{asm}} = \frac{\tau E^2}{\sigma_n^2}, \quad \gamma_{v2,k'}^{\text{asm}} = \frac{\tau E^2}{2K \sigma_n^2}, \quad \gamma_{v3,k'}^{\text{asm}} = \frac{\tau^2 E^4}{\tau E^2 \sigma_n^2 + 2K \tau E^2 \sigma_n^2 + 2K \sigma_n^4},$$

respectively.

Comparing $\gamma_{v1,k'}^{\text{asm}}$, $\gamma_{v2,k'}^{\text{asm}}$ and $\gamma_{v3,k'}^{\text{asm}}$, it can be clearly observed that the asymptotic SINR in Case B-I is the highest, but in Case B-III is the lowest. Thus, the greatest asymptotic SE is observed in Case B-I, but the worst asymptotic SE is observed in Case B-III.

Remark 7. With perfect CSI, recalling $\mathbf{g}_k \sim \mathcal{CN}(0, \eta_k \mathbf{1}_N)$ and $\hat{\mathbf{g}}_k \sim \mathcal{CN}(0, \frac{P_P \eta_k^2}{P_P \eta_k + 1} \mathbf{1}_N)$, we have $\eta_k = \frac{P_P \eta_k^2}{P_P \eta_k + 1}$. Therefore, the asymptotic SINR $\gamma_{k'}$ in (23) becomes (22).

4 Approximation of spectral efficiency

In this section, we present the approximate expression on the SE in the considered system. The achievable rate at user k' in pair (k, k') is given by

$$R_{k'} = \frac{T - \tau}{2T} \mathbb{E} \{ \log_2(1 + \gamma_{k'}) \}. \quad (30)$$

Using the Jansen inequality, we obtain

$$R_{k'} \geq \tilde{R}_{k'} \equiv \frac{T - \tau}{2T} \log_2 \left(1 + [E_{k'}]^{-1} \right), \quad (31)$$

where

$$E_{k'} \triangleq \mathbb{E} \{ [\gamma_{k'}]^{-1} \}. \quad (32)$$

Recalling that the i th communication pair is represented by $(2i - 1, 2i)$, $i = 1, \dots, K$, we have the following Theorem 3.

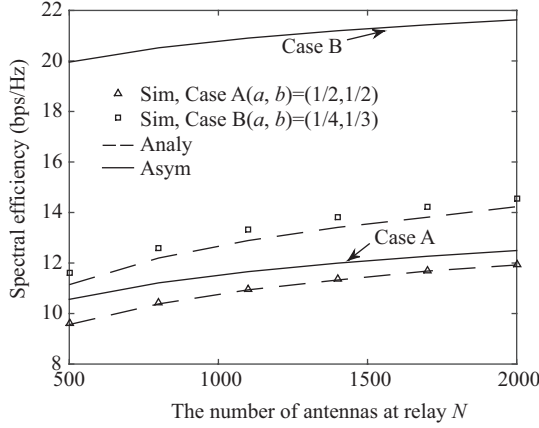
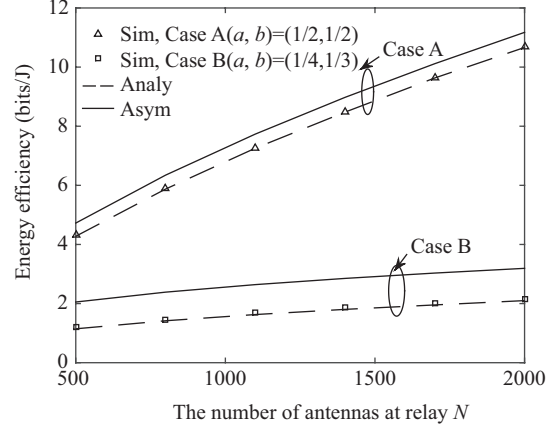
Theorem 3. An approximation of the spectral efficiency in the considered system is given by

$$\tilde{R}_{\text{sum}} \approx \sum_{i=1}^K \frac{T - \tau}{2T} \left[\log_2 \left(1 + \frac{NP_U(\eta_{2i-1} - \sigma_{e_{2i-1}}^2)}{\sigma_n^2(1 + A_{2i-1})} \right) + \log_2 \left(1 + \frac{NP_U(\eta_{2i} - \sigma_{e_{2i}}^2)}{\sigma_n^2(1 + A_{2i})} \right) \right], \quad (33)$$

where $\sigma_{e_i}^2$, $i = 1, \dots, 2K$ is given in (6),

$$A_{2i-1} = \frac{P_U \varphi_2 + \varphi_1 \sigma_n^2 / N}{P_R (\eta_{2i-1} - \sigma_{e_{2i-1}}^2) (\eta_{2i} - \sigma_{e_{2i}}^2)^2}, \quad A_{2i} = \frac{P_U \varphi_2 + \varphi_1 \sigma_n^2 / N}{P_R (\eta_{2i} - \sigma_{e_{2i}}^2) (\eta_{2i-1} - \sigma_{e_{2i-1}}^2)^2}, \quad (34)$$

φ_1 and φ_2 are given as in (16) and (17), respectively.


Figure 2 The SE P_P versus N with imperfect CSI.

Figure 3 The EE versus N with imperfect CSI.

Proof. See Appendix B.

Theorem 3 presents the approximate expression on the SE in the considered system. It can be observed that \tilde{R}_{sum} increases as N increases or as the channel estimation error in all links reduces, but decreases as A_{2i-1} or A_{2i} increases.

5 Numerical and simulation results

In this section, the numerical and Monte-Carlo simulation results are presented to evaluate the SE and EE in the considered system. In Figures 2–8, “Sim” denotes the abbreviation of simulation, “Asym” represents the asymptotic results obtained from Theorems 1 and 2, and “Analy” is short for the approximate results obtained from Theorem 3. We assume that $E_U = E_R = 10$, all noise variance $\sigma_n^2 = 1$, the coherence interval $T = 200$, the number of communication pairs $K = 2$. We also assume that the system structure is symmetric, i.e., $\eta_i = 1$, $\sigma_{e_i}^2 = \sigma_e^2 = 0.1$, $i = 1, \dots, 2K$. For variable P_P , the length of pilot sequences $\tau = 2K$, and $P_P = \tau P_U$.

Firstly, we consider Case A ($a = 1/2$, $b = 1/2$) for fixed P_P and Case B ($a = 1/4$, $b = 1/3$) for variable P_P . With imperfect CSI, Figures 2 and 3 compare the simulated SE and EE with the analytical and asymptotic results for the fixed P_P and variable P_P , respectively. From Figures 2 and 3, it can be observed for fixed and variable P_P , the SE and EE both increase as $N \rightarrow \infty$, which is reasonable since the asymptotic $\gamma_{k'}$ s grow with the increase of N . In addition, as $N \rightarrow \infty$, it shows that our asymptotic and analytical SE/EE become very tight, indicating the validity of our analysis. Furthermore, as expected, it can be seen that for the deeper power scaling, the SE in Case A for fixed P_P is lower than that in Case B for variable P_P , while the EE in Case A for fixed P_P is comparatively greater than that in Case B for variable P_P . For example, when $N = 2000$, the SE in Case A is about 2.2 bps/Hz less than that in Case B, while the EE in Case A is about 8.6 bits/J greater than that in Case B.

In Figures 4–6, we consider three power scaling cases for fixed P_P , i.e., Case A-I ($a = 1, b = 0$), Case A-II ($a = 0, b = 1$) and Case A-III ($a = 1, b = 1$). Figure 4 shows the SE versus the number of relay antennas N for fixed P_P with perfect/imperfect CSI. From Figure 4, it can be seen that when N increases, the SE tends to a certain constant value for perfect/imperfect CSI, respectively, which is consistent with our analysis, since the asymptotic $\gamma_{k'}$ converges to a constant. For example, considering Case A with $a = 1, b = 0$, SE converges to 6.7 bps/Hz with perfect CSI and 6.3 bps/Hz with imperfect CSI. We can also clearly observe that all analytical and asymptotic results are very tight at large N . As expected, the SE with perfect CSI performs better than that with imperfect CSI. For example, there is about 0.4 bps/Hz gap in SE between perfect and imperfect CSI cases in Case A with $a = 1, b = 0$. Besides, it can be seen that the SE in Case A-I is the maximal among the above three power scaling cases for fixed P_P , which is consistent with Remark 2. From Remarks 3 and 7, it is shown that the asymptotic $\gamma_{k'}$ for

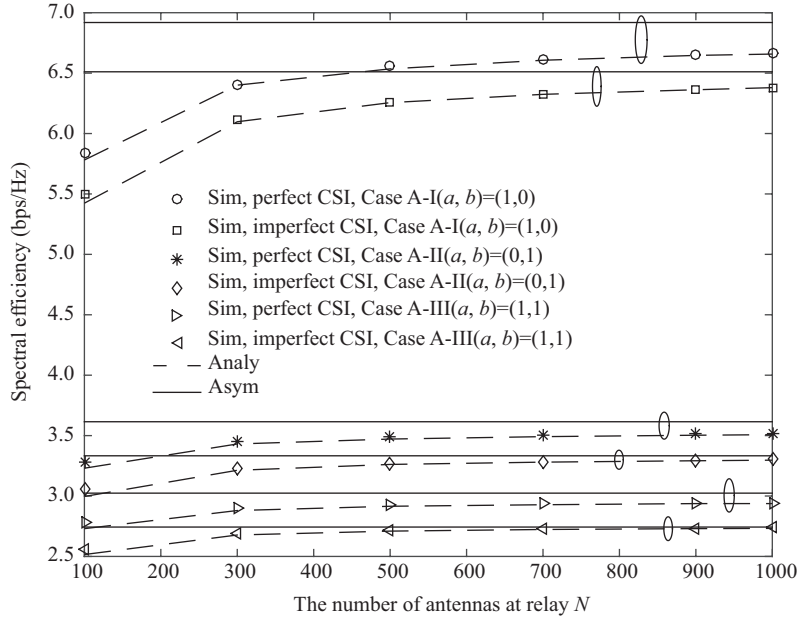


Figure 4 The SE for fixed P_P versus N with perfect/imperfect CSI.

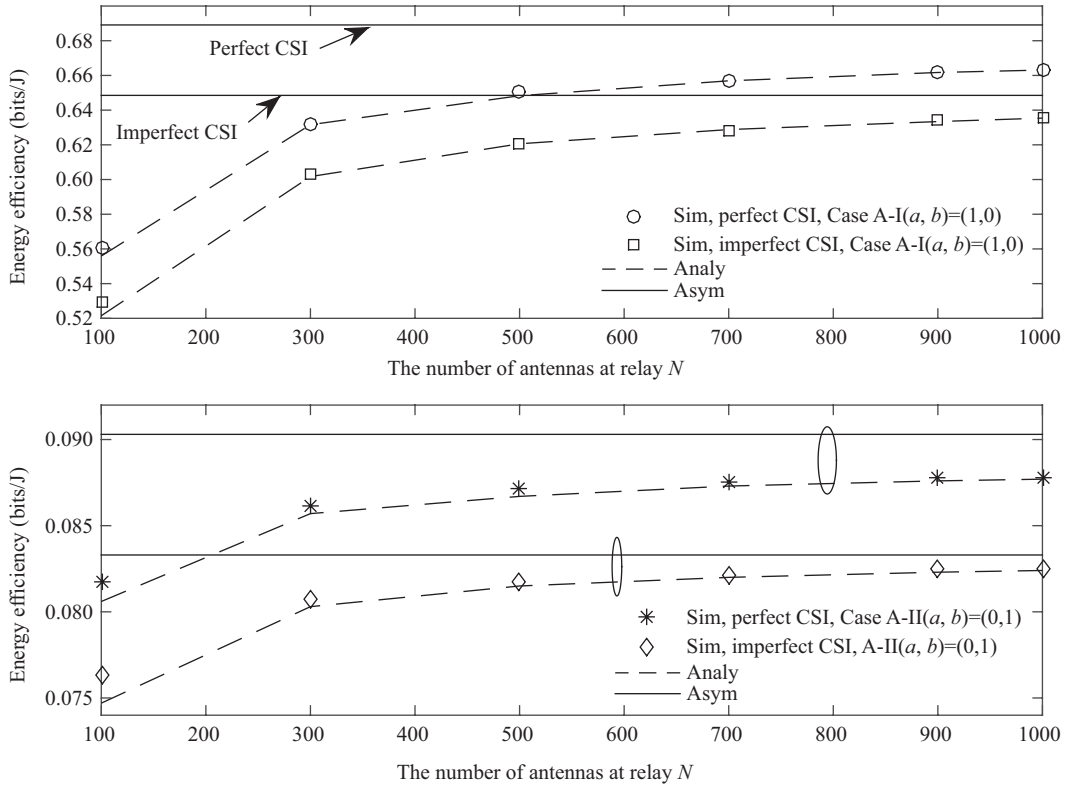


Figure 5 Case A-I and A-II: The EE versus N with perfect/imperfect CSI.

fixed P_P is identical with the one for variable P_P with perfect CSI. Thus, due to the space limitation, here, we only compare the SE and EE with perfect/imperfect CSI for fixed P_P , which is reasonable.

Figure 5 compares the EE for perfect/imperfect CSI in Case A-I and Case A-II. It can be clearly seen that when $N \rightarrow \infty$, the EE approaches to a constant value, which is consistent with the conclusion in (14). For example, considering Case A-I with $a = 1, b = 0$, the EE converges to 0.66 bits/J with perfect CSI while 0.64 bits/J with imperfect CSI. It can be seen that for both perfect/imperfect CSI, the analytical

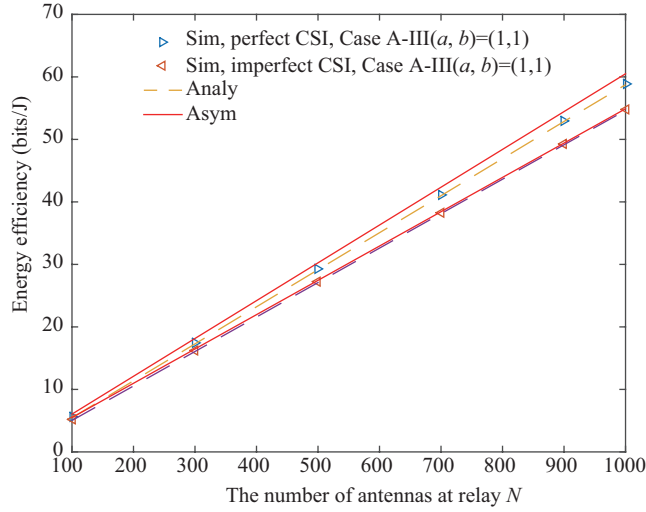


Figure 6 (Color online) Case A-III: The EE versus N with perfect/imperfect CSI.

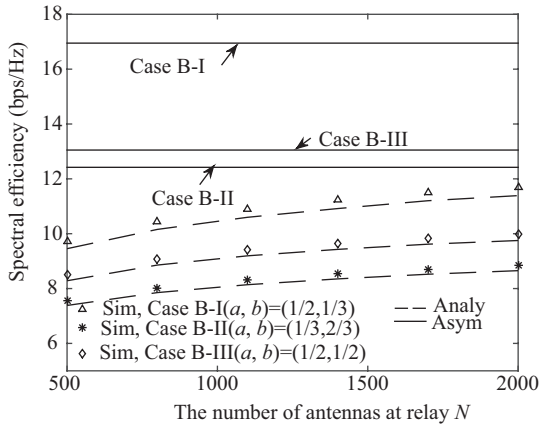


Figure 7 The SE versus N with imperfect CSI.

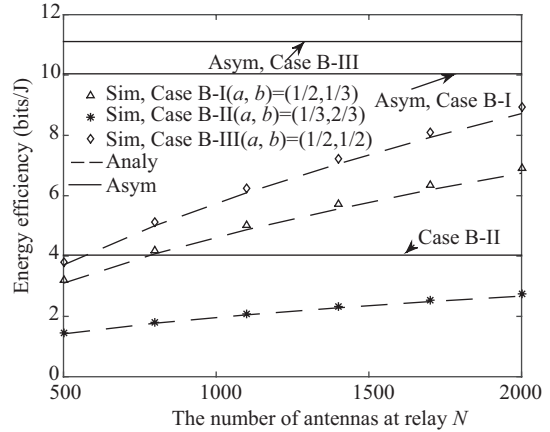


Figure 8 The EE versus N with imperfect CSI.

EE is very close to the simulated ones when N is very large. Moreover, Figure 6 shows the EE for perfect/imperfect CSI in Case A-III. Again, it can be observed that the analytical and asymptotic results are very tight, as $N \rightarrow \infty$. Notably, the EE grows linearly with N for perfect/imperfect CSI, which is also reasonable due to (14). From Figures 5 and 6, it is shown that the EE with perfect CSI outperforms the counterpart with imperfect CSI, that is to say, the EE is impaired by the channel estimation errors.

Next, in Figures 7 and 8, we consider the three power scaling cases for variable P_P with imperfect CSI, i.e., Case B-I ($a = 1/2, b = 1/3$), Case B-II ($a = 1/3, b = 2/3$) and Case B-III ($a = 1/2, b = 1/2$). In Figure 7, it is illustrated that the analytical SE results approximate the simulated ones very well, especially when N is large. Additionally, all simulation results approach to their asymptotic results, as $N \rightarrow \infty$. Furthermore, it is easily observed that Case B-I performs the best among the three power cases, which is consistent with Remark 6. In Figure 8, the simulated EE also approaches to the fixed value as N becomes large. Thus, the tightness of analytical results is verified.

6 Conclusion

In this paper, considering the fixed P_P and the variable P_P , the SE and the EE performance were investigated for a massive MIMO multi-pair two-way AF relaying system, with general power scaling schemes and imperfect CSI. In a large relaying antenna regime, we firstly obtained the asymptotic expression of

the SINR, from which the asymptotic SE and EE were deduced. Furthermore, we derived an approximate closed-form expression of the SE. As the antenna number of relay station grows without bound, our analysis results revealed that the transmit power at each user and relay station can be scaled down by $1/N$ with fixed P_P , but can be further cut down by $1/\sqrt{N}$ with variable P_P . Numerical results accompanied with Monte-Carlo simulations verified the accuracy of the proposed mathematical analysis.

Acknowledgements This work was supported by National Natural Science Foundation of China (Grant Nos. 61301111, 61472343) and China Postdoctoral Science Foundation (Grant No. 2014M56074).

Conflict of interest The authors declare that they have no conflict of interest.

References

- 1 Wang D M, Zhang Y, Wei H, et al. An overview of transmission theory and techniques of large-scale antenna systems for 5G wireless communications. *Sci China Inf Sci*, 2016, 59: 081301
- 2 Ma Z, Zhang Z Q, Ding Z G, et al. Key techniques for 5G wireless communications: network architecture, physical layer, and MAC layer perspectives. *Sci China Inf Sci*, 2015, 58: 041301
- 3 Larsson E, Edfors O, Tufvesson F, et al. Massive MIMO for next generation wireless systems. *IEEE Commun Mag*, 2014, 52: 186–195
- 4 Yang A, Xing C W, Fei Z S, et al. Performance analysis for uplink massive MIMO systems with a large and random number of UEs. *Sci China Inf Sci*, 2016, 59: 022312
- 5 Zhang Q, Jin S, Wong K K, et al. Power scaling of uplink massive MIMO systems with arbitrary-rank channel means. *IEEE J Sel Signal Process*, 2014, 8: 966–981
- 6 Ngo H Q, Larsson E, Marzetta T. Energy and spectral efficiency of very large multiuser MIMO systems. *IEEE Trans Commun*, 2013, 61: 1436–1449
- 7 Han B, Zhao S, Yang B, et al. Historical PMI based multi-user scheduling for FDD massive MIMO systems. In: *Proceedings of the IEEE Vehicular Technology Conference (VTC)*, Nanjing, 2016. 1–5
- 8 Yang J, Fan P, Duong T Q, et al. Exact performance of two-way AF relaying in Nakagami- m fading environment. *IEEE Trans Wirel Commun*, 2011, 10: 980–987
- 9 Zhang H J, Xing H, Cheng J L, et al. Secure resource allocation for OFDMA two-way relay wireless sensor networks without and with cooperative jamming. *IEEE Trans Ind Inf*, 2016, 12: 1714–1725
- 10 Cui H, Song L Y, Jiao B L. Multi-pair two-way amplify-and-forward relaying with very large number of relay antennas. *IEEE Trans Wirel Commun*, 2014, 13: 2636–2645
- 11 Jin S, Liang X, Wong K K, et al. Ergodic rate analysis for multipair massive MIMO two-way relay networks. *IEEE Trans Wirel Commun*, 2014, 14: 1480–1491
- 12 Dai Y, Dong X. Power allocation for multi-pair massive MIMO two-way AF relaying with linear processing. *IEEE Trans Wirel Commun*, 2016, 15: 5932–5946
- 13 Ngo H Q, Suraweera H, Matthaiou M, et al. Multipair full-duplex relaying with massive arrays and linear processing. *IEEE J Sel Areas Commun*, 2014, 32: 1721–1737
- 14 Zhang Z S, Wang X, Zhang C Y, et al. Massive MIMO technology and challenges (in Chinese). *Sci Sin Inform*, 2015, 45: 1095–1110
- 15 Xue Y, Zhang J, Gao X Q. Resource allocation for pilot-assisted massive MIMO transmission. *Sci China Inf Sci*, 2017, 60: 042302
- 16 Khansefid A, Hlaing M. Asymptotically optimal power allocation for massive MIMO uplink. In: *Proceedings of the IEEE International Conference on Signal and Information Processing (GlobalSIP)*, Atlanta, 2014. 627–631
- 17 Dong Y, Qiu L. Closed-form ASE of downlink massive MIMO system with uplink and downlink training. In: *Proceedings of the IEEE International Conference on Wireless Communications Signal Processing (WCSP)*, Nanjing, 2015. 1–5
- 18 Yang A, He Z, Xing C, et al. The role of large-scale fading in uplink massive MIMO systems. *IEEE Trans Veh Tech*, 2016, 65: 477–483
- 19 Yang J, Wang H Y, Ding J, et al. Spectral and energy efficiency for massive MIMO multi-pair two-way relay networks with ZFR/ZFT and imperfect CSI. In: *Proceedings of Asia-Pacific Conference on Communications (APCC)*, Kyoto, 2015. 47–51
- 20 Kong C, Zhong C J, Papazafeiropoulos A K, et al. Sum-rate and power scaling of massive MIMO systems with channel aging. *IEEE Trans Commun*, 2015, 63: 4879–4893
- 21 Silva S, Amarasuriya G, Tellambura C, et al. Massive MIMO two-way relay networks with channel imperfections. In: *Proceedings of the IEEE International Conference on Communications (ICC)*, Kuala Lumpur, 2016. 1–7
- 22 Xing C W, Ma S D, Zhou Y Q. Matrix-monotonic optimization for MIMO systems. *IEEE Trans Signal Process*, 2015, 63: 334–348
- 23 Cramér H. *Random Variables and Probability Distributions*. Cambridge: Cambridge University Press, 1970

Appendix A Proof of Theorem 1

According to the law of large numbers, we obtain

$$\frac{1}{N} \hat{\mathbf{g}}_k^T \mathbf{e}_k \xrightarrow[N \rightarrow \infty]{\text{a.s.}} 0, \quad \frac{1}{N} \mathbf{e}_k^T \mathbf{e}_{k'} \xrightarrow[N \rightarrow \infty]{\text{a.s.}} 0. \quad (\text{A1})$$

As such, we have

$$P_A \xrightarrow[N \rightarrow \infty]{\text{a.s.}} 0, \quad P_{II} \xrightarrow[N \rightarrow \infty]{\text{a.s.}} 0, \quad P_{SI} \xrightarrow[N \rightarrow \infty]{\text{a.s.}} 0, \quad \text{and} \quad P_N \xrightarrow[N \rightarrow \infty]{\text{a.s.}} \sigma_n^2 \|\hat{\mathbf{g}}_{k'}^T \mathbf{F}\|^2 + \sigma_n^2. \quad (\text{A2})$$

Utilizing (A2), we have

$$\gamma_{k'} \xrightarrow[N \rightarrow \infty]{\text{a.s.}} \frac{P_U |\hat{\mathbf{g}}_{k'}^T \mathbf{F} \hat{\mathbf{g}}_k|^2}{\sigma_n^2 \|\hat{\mathbf{g}}_{k'}^T \mathbf{F}\|^2 + \sigma_n^2}. \quad (\text{A3})$$

Rewriting $\hat{\mathbf{g}}_k \sim \mathcal{CN}(0, \frac{P_P \eta_k^2}{P_P \eta_k + 1} \mathbf{1}_N)$ due to (6), we obtain

$$\hat{\mathbf{g}}_{k'}^T \mathbf{F} \xrightarrow[N \rightarrow \infty]{\text{a.s.}} \beta N (\eta_{k'} - \sigma_{e_{k'}}^2) \hat{\mathbf{g}}_k^H, \quad (\text{A4})$$

and

$$\hat{\mathbf{g}}_{k'}^T \mathbf{F} \hat{\mathbf{g}}_i \xrightarrow[N \rightarrow \infty]{\text{a.s.}} \beta N^2 (\eta_{k'} - \sigma_{e_{k'}}^2) (\eta_i - \sigma_{e_i}^2) \delta_{ki}. \quad (\text{A5})$$

Additionally, using the property $\text{Tr}(\mathbf{AB}) = \text{Tr}(\mathbf{BA})$ and rewriting $[\hat{\mathbf{\Lambda}}]_{kk} = (\eta_k - \sigma_{e_k}^2)$ due to (6), $\text{Tr}(\mathbf{Z}_1)$ and $\text{Tr}(\mathbf{Z}_2)$ in (9) are given by

$$\begin{aligned} \text{Tr}(\mathbf{Z}_1) &\xrightarrow[N \rightarrow \infty]{\text{a.s.}} \text{Tr} \left(N \hat{\mathbf{G}}^T \hat{\mathbf{G}}^* \mathbf{P} \hat{\mathbf{G}}^H \hat{\mathbf{G}} \mathbf{P} \right) \xrightarrow[N \rightarrow \infty]{\text{a.s.}} \text{Tr} \left(N \hat{\mathbf{\Lambda}} \mathbf{P} \hat{\mathbf{\Lambda}} \mathbf{P} \right) \\ &= 2 \sum_{i=1}^K (\eta_{2i-1} - \sigma_{e_{2i-1}}^2) (\eta_{2i} - \sigma_{e_{2i}}^2) N^2 = \varphi_1 N^2, \end{aligned} \quad (\text{A6})$$

$$\begin{aligned} \text{Tr}(\mathbf{Z}_2) &\xrightarrow[N \rightarrow \infty]{\text{a.s.}} \text{Tr} \left(N^2 \hat{\mathbf{G}}^T \hat{\mathbf{G}}^* \mathbf{P} \hat{\mathbf{G}}^H \hat{\mathbf{G}} \hat{\mathbf{G}}^H \hat{\mathbf{G}} \mathbf{P} \right) \xrightarrow[N \rightarrow \infty]{\text{a.s.}} \text{Tr} \left(N^2 \hat{\mathbf{\Lambda}} \mathbf{P} \hat{\mathbf{\Lambda}}^2 \mathbf{P} \right) \\ &= \sum_{i=1}^K (\eta_{2i-1} - \sigma_{e_{2i-1}}^2) (\eta_{2i} - \sigma_{e_{2i}}^2) \left[(\eta_{2i-1} - \sigma_{e_{2i-1}}^2) + (\eta_{2i} - \sigma_{e_{2i}}^2) \right] N^3 = \varphi_2 N^3. \end{aligned} \quad (\text{A7})$$

Therefore, we get

$$\beta^2 \xrightarrow[N \rightarrow \infty]{\text{a.s.}} \frac{P_R}{P_U \varphi_2 N^3 + \varphi_1 \sigma_n^2 N^2}. \quad (\text{A8})$$

Substituting (A4) and (A5) into (A3), we have

$$\gamma_{k'} \xrightarrow[N \rightarrow \infty]{\text{a.s.}} \frac{P_U \beta^2 N^4 (\eta_{k'} - \sigma_{e_{k'}}^2)^2 (\eta_k - \sigma_{e_k}^2)^2}{\sigma_n^2 \beta^2 N^3 (\eta_{k'} - \sigma_{e_{k'}}^2)^2 (\eta_k - \sigma_{e_k}^2) + \sigma_n^2}. \quad (\text{A9})$$

Let $P_U = E_U/N^a$, $P_R = E_R/N^b$, $a, b \geq 0$, substituting (A8) into (A9), Theorem 2 can be deduced.

Appendix B Proof of Theorem 3

Recalling that the SINR at the k' th user, we have

$$\text{E} \left\{ [\gamma_{k'}]^{-1} \right\} = \text{E} \left\{ \frac{P_A + P_N + P_{SI} + P_{II}}{P_U |\hat{\mathbf{g}}_{k'}^T \mathbf{F} \hat{\mathbf{g}}_k|^2} \right\}. \quad (\text{B1})$$

Due to (4), one can obtain

$$\hat{\mathbf{g}}_{k'}^T \mathbf{F} \xrightarrow[N \rightarrow \infty]{\text{a.s.}} \beta \hat{\mathbf{g}}_{k'}^T \hat{\mathbf{g}}_{k'}^* \mathbf{1}_{k'} \mathbf{P} \hat{\mathbf{G}}^H = \beta \|\hat{\mathbf{g}}_{k'}\|^2 \hat{\mathbf{g}}_k^H, \quad (\text{B2})$$

and

$$\hat{\mathbf{g}}_{k'}^T \mathbf{F} \hat{\mathbf{g}}_i \xrightarrow[N \rightarrow \infty]{\text{a.s.}} \beta \|\hat{\mathbf{g}}_{k'}\|^2 \|\hat{\mathbf{g}}_i\|^2 \delta_{ki}. \quad (\text{B3})$$

Consequently, recalling (A2) and substituting (B2) and (B3) into (B1) we have

$$\begin{aligned} \text{E} \{ [\gamma_{k'}]^{-1} \} &\xrightarrow[N \rightarrow \infty]{\text{a.s.}} \text{E} \left\{ \frac{\sigma_n^2 \beta^2 \|\hat{\mathbf{g}}_{k'}\|^4 \|\hat{\mathbf{g}}_k\|^2 + \sigma_n^2}{P_U \beta^2 \|\hat{\mathbf{g}}_{k'}\|^4 \|\hat{\mathbf{g}}_k\|^4} \right\} \\ &= \frac{\sigma_n^2}{P_U} \text{E} \left\{ \frac{1}{\|\hat{\mathbf{g}}_k\|^2} \right\} + \frac{\sigma_n^2}{P_U \beta^2} \text{E} \left\{ \frac{1}{\|\hat{\mathbf{g}}_k\|^4} \right\} \cdot \text{E} \left\{ \frac{1}{\|\hat{\mathbf{g}}_{k'}\|^4} \right\}. \end{aligned} \quad (\text{B4})$$

Utilizing the properties of Wishart matrix, we obtain

$$\text{E} \left\{ \frac{1}{\|\hat{\mathbf{g}}_k\|^2} \right\} = \frac{1}{(N-1)(\eta_k - \sigma_{e_k}^2)} \approx \frac{1}{N(\eta_k - \sigma_{e_k}^2)}, \quad (\text{B5})$$

and

$$\begin{aligned} \mathbb{E} \left\{ \frac{1}{\|\hat{\mathbf{g}}_k\|^4} \right\} \cdot \mathbb{E} \left\{ \frac{1}{\|\hat{\mathbf{g}}_{k'}\|^4} \right\} &= \frac{1}{(N-1)^2 (N-2)^2 (\eta_k - \sigma_{e_k}^2)^2 (\eta_{k'} - \sigma_{e_{k'}}^2)^2} \\ &\approx \frac{1}{N^4 (\eta_k - \sigma_{e_k}^2)^2 (\eta_{k'} - \sigma_{e_{k'}}^2)^2}. \end{aligned} \tag{B6}$$

Substituting (B5), (B6) and (A8) into (B4), we have

$$\begin{aligned} \mathbb{E}\{[\gamma_{k'}]^{-1}\} &\stackrel{\text{a.s.}}{N \rightarrow \infty} \frac{\sigma_n^2}{P_U} \frac{1}{(N-1)(\eta_k - \sigma_{e_k}^2)} + \frac{\sigma_n^2}{P_U \beta^2} \frac{1}{(N-1)^2 (N-2)^2 (\eta_k - \sigma_{e_k}^2)^2 (\eta_{k'} - \sigma_{e_{k'}}^2)^2} \\ &\approx \frac{1}{N} \cdot \frac{\sigma_n^2}{P_U} \frac{1}{(\eta_k - \sigma_{e_k}^2)} + \frac{1}{N^4} \cdot \frac{1}{\beta^2} \cdot \frac{\sigma_n^2}{P_U} \cdot \frac{1}{(\eta_k - \sigma_{e_k}^2)^2 (\eta_{k'} - \sigma_{e_{k'}}^2)^2} \\ &\stackrel{\text{a.s.}}{N \rightarrow \infty} \frac{\sigma_n^2}{NP_U} \left\{ \frac{1}{(\eta_k - \sigma_{e_k}^2)} + \frac{(P_U \varphi_2 N^3 + \varphi_1 \sigma_n^2 N^2)}{P_R (\eta_k - \sigma_{e_k}^2)^2 (\eta_{k'} - \sigma_{e_{k'}}^2)^2 N^3} \right\} \\ &= \frac{\sigma_n^2}{NP_U (\eta_k - \sigma_{e_k}^2)} \left\{ 1 + \frac{P_U \varphi_2 + \varphi_1 \sigma_n^2 / N}{P_R (\eta_k - \sigma_{e_k}^2) (\eta_{k'} - \sigma_{e_{k'}}^2)^2} \right\}. \end{aligned} \tag{B7}$$

Substituting (B7) into (32) and using (13), Theorem 3 can be deduced.